

# Effects of the Precipitation pH of Sodium Silicate on the Amorphous Silica Characteristics and its capability in the Pb and Cd Adsorption

Maryani Eneng\*, Septawendar Rifki and Suhanda

Department of Advanced Ceramics, Glass and Enamel, Center for Ceramics, Ministry of Industry of Indonesia, Bandung 40272, INDONESIA

\*maryani\_eneng@yahoo.co.id

## Abstract

*Amorphous silica was successfully synthesized from sodium silicate solution as a precursor by a precipitation method using sulfuric acid solution. It was precipitated at various pH conditions of about 4, 7 and 9. The silica was characterized by X-ray diffraction, Fourier Transform Infra-red (FT-IR) and Scanning electron microscopy studies. Meanwhile, the textural properties of the silica such as specific surface area, pore diameter and pore distribution were measured with Brunauer-Emmett-Teller method. The X-ray diffraction results demonstrate all the silica samples exhibiting a low-intensity broad peak at a diffraction angle  $2\theta$  of  $21.8^\circ$ , indicating an amorphous structure.*

*The microstructure investigation shows the formation of nanoparticle amorphous silica at all pH conditions. The infra-red analysis results show that the precipitated amorphous silica at pH 9 still contained carbonate. However, the carbonate group causes the amorphous silica to exhibit the surface area of  $84 \text{ m}^2/\text{g}$ , which is lower than those precipitated under neutral and acidic conditions. The result of the study indicated that the precipitated amorphous silica at pH 4 has the highest surface area and total pore volume of  $436 \text{ m}^2/\text{g}$  and  $0.91 \text{ cc/g}$  respectively; and the smallest average pore diameter of  $8.4 \text{ nm}$ . However, the basic precipitated silica has the highest % adsorption of the Pb(II) and Cd(II) heavy metals of about 98% at a contact time of 24 hours.*

**Keywords:** Sodium silicate precursor, amorphous silica, the precipitation pH, surface area, heavy metal adsorption.

## Introduction

Precipitated silica has been found to be compatible in a wide range of materials and performs excellent functions; for instance, serving as an inert and reinforcing filler in rubber, plastics, dielectric materials, flat panel displays, sensors, as well as for filter in exhaust gases, adsorbents, drug delivery systems, anticorrosion agent and heterogeneous catalysts in various chemical reactions<sup>1-7</sup>. This material can be produced from precursors such as silica sand, silica fumed, alkyl ortho-silicates and sodium silicates. Among them, sodium silicate (water-glass) is the more economical and

environmentally-friendly source of silica because this precursor is cheap, aqueous solvent-based and a good source for a large-scale production of precipitated silica<sup>1-2</sup>.

The precipitated silica characteristic is controlled by several synthesis parameters such as reactant concentrations, synthesis temperatures, time of precipitation, pH the addition and kind of surfactants, solvents and a method of washing and drying<sup>1,3-5</sup>. These parameters influence the final  $\text{SiO}_2$  characteristics such as the size and uniformity particles, the morphology and the aggregation, a pore diameter, a total pore volume and a specific surface area.

The aim of this work is to study the effect of the pH parameter on the amorphous silica properties obtained from the sodium silicate precursor and to investigate its capability on the heavy metal adsorption such as Pb and Cd.

## Material and Methods

**Materials:** The materials used in this work were commercial aqueous solution of sodium silicate with  $\text{SiO}_2$  concentration of 25%, sulfuric acid solution from Merck Inc. and commercial sodium carbonate. All of the said materials were used without further purification.

**Synthesis of Amorphous Silica:** An amorphous silica was prepared by neutralizing 20 % (v/v) of sodium silicate solution with a sulfuric acid solution until the final pH 7 was achieved, resulting in white precipitates. This precipitated silica was filtered and subsequently washed with distilled water. It was then dried in an oven at a temperature of  $100^\circ\text{C}$  and labeled as neutral silica.

An acid silica was obtained by adding an excess of sulfuric acid solution to the precipitated silica until it reaches a pH of 4. Then, it was filtered and dried at a temperature of  $100^\circ\text{C}$ . Meanwhile, a basic silica was produced by mixing a 10% (w/v)  $\text{Na}_2\text{CO}_3$  solution to the neutral silica until the final pH of the mixture was 9. This precipitated silica was filtered, subsequently washed with distilled water and dried at a temperature of  $100^\circ\text{C}$ .

**Adsorption Pb and Cd by the precipitated silica:** Each 10 grams of the acidic, neutral and basic silica are respectively suspended in two 250 mL standard solutions containing 12 ppm Pb and 14 ppm Cd respectively. The mixture was stirred for 1 hour and aged with time variations of 7, 17 and 23 hours. Then the precipitated silica was filtered and the filtrates were measured with an AAS instrument for analyzing the concentration change of Pb and Cd metals.

**Characterization:** A Prestige 21 Shimadzu Fourier Transform Infra-red (FT-IR) spectrophotometer was used to analyze the infra-red spectra of all the precipitated silica. The phase composition of the precipitated silica was identified by X-Ray Diffraction (XRD) instrument using a PANalytical X'Pert PRO X-ray diffractometer at 40 Kv and 30 mA with a Cu/K $\alpha$  ( $\lambda = 1.54060 \text{ \AA}$ ) radiation source. The morphologies of all the precipitated silica were observed using a JEOL JSM-35C Scanning Electron Microscope (SEM). The textural properties of the silica were measured by a Quantachrome NovaWin instrument through a Brunauer-Emmett-Teller (BET) method. The heavy metal concentrations of Pb and Cd were measured using a Varian SpectraAA 55B Atomic Absorption Spectrometer (AAS).

## Results and Discussion

**Infra-red characteristics of precipitated silica:** Fig. 1 shows the FT-IR spectra of the precipitated silica under acidic, neutral and basic conditions. All precipitated silica shows the peaks of amorphous silica such as an IR band at  $3437 \text{ cm}^{-1}$  could be assigned to the stretching vibration of the  $\text{H}_2\text{O}$  molecules; the band at  $1627.92\text{-}1635.64 \text{ cm}^{-1}$  is due to bending vibration of the  $\text{H}_2\text{O}$  molecules; and a broad band in the range of  $3670\text{-}3000 \text{ cm}^{-1}$  is responsible for the surface  $-\text{OH}$  groups of Si-OH; the shoulder at  $3246 \text{ cm}^{-1}$  is due the stretching vibrations of Si-OH groups in the structure of amorphous silica; the band at  $1103.28 \text{ cm}^{-1}$  originates from the Si-O-Si asymmetric stretching vibration; the band at  $964.41\text{-}972.12 \text{ cm}^{-1}$  is due to the silanol groups, the Si-O stretching vibrations and the band at  $802.39 \text{ cm}^{-1}$  is responsible for the Si-O-Si symmetric stretching vibrations<sup>5,8-10</sup>.

The IR band at  $462.92 \text{ cm}^{-1}$  was detected in the acidic and neutral precipitated silica but it is recorded as a shoulder in the IR spectrum of the basic silica. This band indicates the presence of O-Si-O bending vibrations<sup>5</sup>. The IR bands in the range of  $470\text{-}450 \text{ cm}^{-1}$  could be assigned to the Si-O asymmetric bending vibration of Si-O-Si<sup>9</sup>.

These IR spectra were measured at  $400\text{-}4000 \text{ cm}^{-1}$ , thus the bands at  $354.9 \text{ cm}^{-1}$  and  $316\text{-}380 \text{ cm}^{-1}$  originating from Si-OH vibrations<sup>5</sup> cannot be identified. However, the band at  $3246 \text{ cm}^{-1}$  which denotes the Si-OH vibration on the basic silica is more tapered than the others. These results prove that basic silica contains higher hydroxyl groups of Si-OH than other silica types.

The bands at  $794.67 \text{ cm}^{-1}$  and  $2931.80 \text{ cm}^{-1}$  are only detected on basic silica. These bands are due to carbonate group. The small shoulders at  $1135, 998$  and  $613 \text{ cm}^{-1}$  are attributed to sulphate absorptions<sup>11</sup>. These bands were detected on all precipitated silica.

**Mineralogy characteristics of the precipitated silica:** Fig. 2 represents the XRD pattern of all the precipitated silica. The XRD results show a broad peak at the diffraction angle  $2\theta$  of  $21.8^\circ$  in all the precipitated silica indicating the

formation of amorphous silica<sup>5</sup>. The existence of sulfate, hydroxyl and carbonate groups in the acid, neutral and basic precipitated silica respectively, is the characteristics of the amorphous structure. There are two unidentified peaks of  $44.5^\circ$  and  $32^\circ$  angles that were detected in basic silica.

**Morphology of precipitated silica:** Fig. 3 shows the typical SEM images of the nanosized amorphous silica precipitated at various pH conditions. The morphologies of the acidic and neutral precipitated silica are more agglomerated and dense compared to the basic precipitated silica.

Amorphous silica is easy to agglomerate because of its high surface area and the presence of free OH groups on its surface, resulting in the hydrogen bond with water molecules. This hydrogen bond was removed, forming siloxane (Si-O-Si) when the dispersed silica was isolated from the solvent resulting in larger sized particles that were agglomerated<sup>8,10</sup>.

Sodium silicate  $[(\text{SiO}_2)_n.\text{Na}_2\text{O}, n < 4]$  that was used as a precursor for synthesis of precipitated silica has the initial pH in the range of  $11\text{-}13$ <sup>12</sup>. The addition of sulfuric acid to sodium silicate solution will form the silicic acid  $(\text{Si}(\text{OH})_4)$  which subsequently undergoes polymerization of silanol group (Si-OH) to siloxane bonds (Si-O-Si) and finally settles as precipitated silica. In general, silicic acid tends towards a maximum number of siloxane bonds and minimum number of uncondensed silanol (Si-OH) groups<sup>6</sup>. As a result, early polymerization leads to ring structures together with cyclic polymers causing the final larger three-dimensional solid particles with morphology tending to be rounded as indicated by the acidic and neutral silica.

The morphology of the basic silica is branched clusters, less agglomerated and more porous. This is due to the addition of sodium carbonate compounds to this silica which inhibits the formation of siloxane due to charge screening by the effect of salinity<sup>12</sup>. Therefore, the basic silica contains more silanol group as shown in FTIR results in fig. 1.

**Textural Characteristics:** According to the International Union of Pure and Applied Chemistry (IUPAC)<sup>13</sup>, a pore size of the acidic, neutral and basic silica is classified into meso pores with pore sizes of between 2 and 50 nm, as shown in table 1. The basic silica has the largest pore size of 36.2 nm. This result is consistent with the morphology of this silica which is more porous than the other silica in fig. 2.

The acidic silica has the highest surface area and a total pore volume of  $436 \text{ m}^2/\text{g}$  and  $0.91 \text{ cc/g}$  respectively, but it shows the smallest average pore diameter of 8.4 nm as shown in Table 1. Otherwise, the basic silica has the smallest surface area of  $84 \text{ m}^2/\text{g}$ .

**Adsorption Pb and Cd ions:** Lead (Pb) and cadmium (Cd) belong to the group of serious hazardous heavy metals

because it is so toxic<sup>14</sup>. Adsorption is one of the most commonly used methods to eliminate the exposure of both heavy metals from aqueous media. In this study, the precipitated silica at various pH conditions was used as adsorbents.

Fig. 4 shows that the % adsorption of Pb(II) by the precipitated silica increased up to 20 hours except for the basic silica that was still increasing. Further increase in contact time did not change the % of adsorption, indicating the attainment of quasi equilibrium state for neutral silica adsorbent, even the percentage adsorption of the Pb ion has decreased for the acidic silica.

The results show that the order of Pb ion adsorption was acid<neutral<basic silica adsorbent. This is due to the fact that precipitated silica at higher pH will contain more silanol (Si-OH) groups. At pH 6.0, the silanols are partially deprotonated, generating negatively charged SiO<sup>-</sup> groups that can interact with the metal Pb cations by electrostatic attractions<sup>15</sup>. Pb ion adsorption capacity of basic silica is much greater than other silica which adsorbed Pb ion by 98.56% in the course of 24 hours of contact time. This is due to the adsorption of Pb ion by SiO<sup>-</sup> and carbonate groups that

were present in the basic silica. The carbonate group may lead the basic silica to interact strongly with the Pb ions as ligands and form a complex compound.

The adsorption of Cd(II) curve of the precipitated silica shows a pattern that is similar to the Pb ion adsorption curve as shown in figs. 4 and 5. The results show that the order of Cd ion adsorption was acid<neutral<basic silica adsorbent, but the Cd(II) adsorption capacity of the acid and neutral silica shows the curves that coincide.

Tables 2 and 3 show that all precipitated silica have higher adsorption capacity to Pb ions compared to Cd ions. The ionic radii of Pb and Cd are 0.118 and 0.097 nm respectively.<sup>14</sup> Normally, cations with larger ionic radii preferentially displace cations with smaller ionic radii. Based on ionic radii, the order of silica bonding preference should have been: Pb(II) > Cd(II).

Figs. 6 and 7 shows that the specific adsorption of the Pb and Cd ions decrease when increasing the retention time. This is due to the declining population of the remaining Pb and Cd ions at a longer retention time.

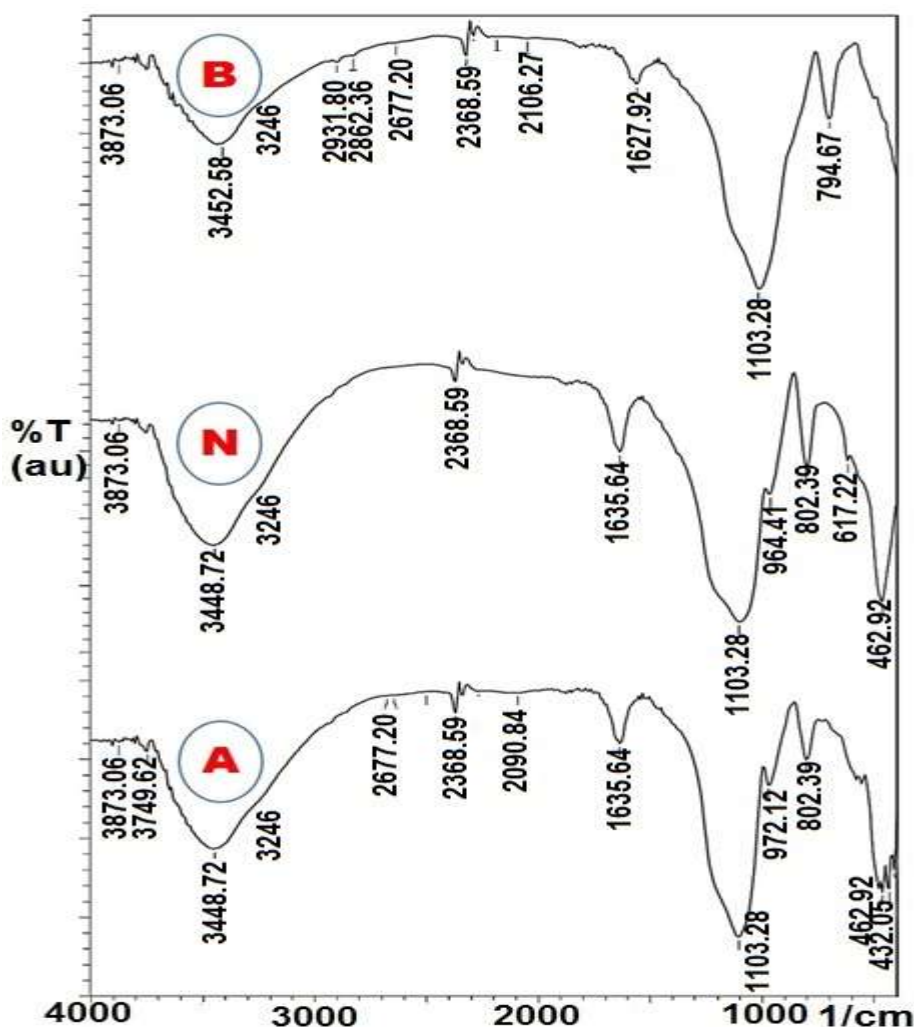


Figure 1: FT-IR spectrum of precipitated SiO<sub>2</sub> (A) acid; (N) neutral and (B) basic

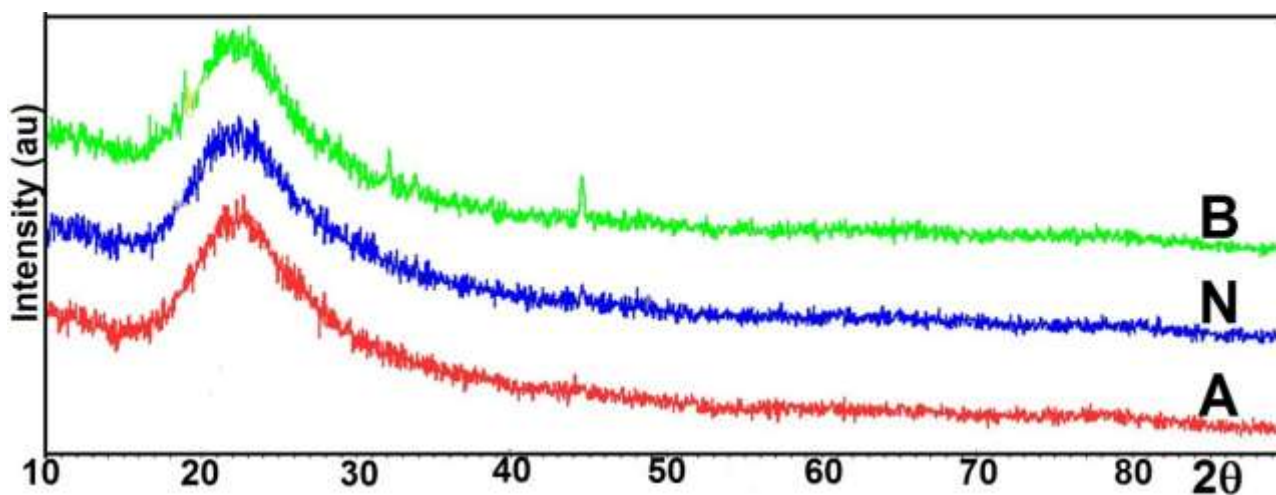


Figure 2: XRD pattern of precipitated SiO<sub>2</sub> (A) acid; (N) neutral and (B) basic

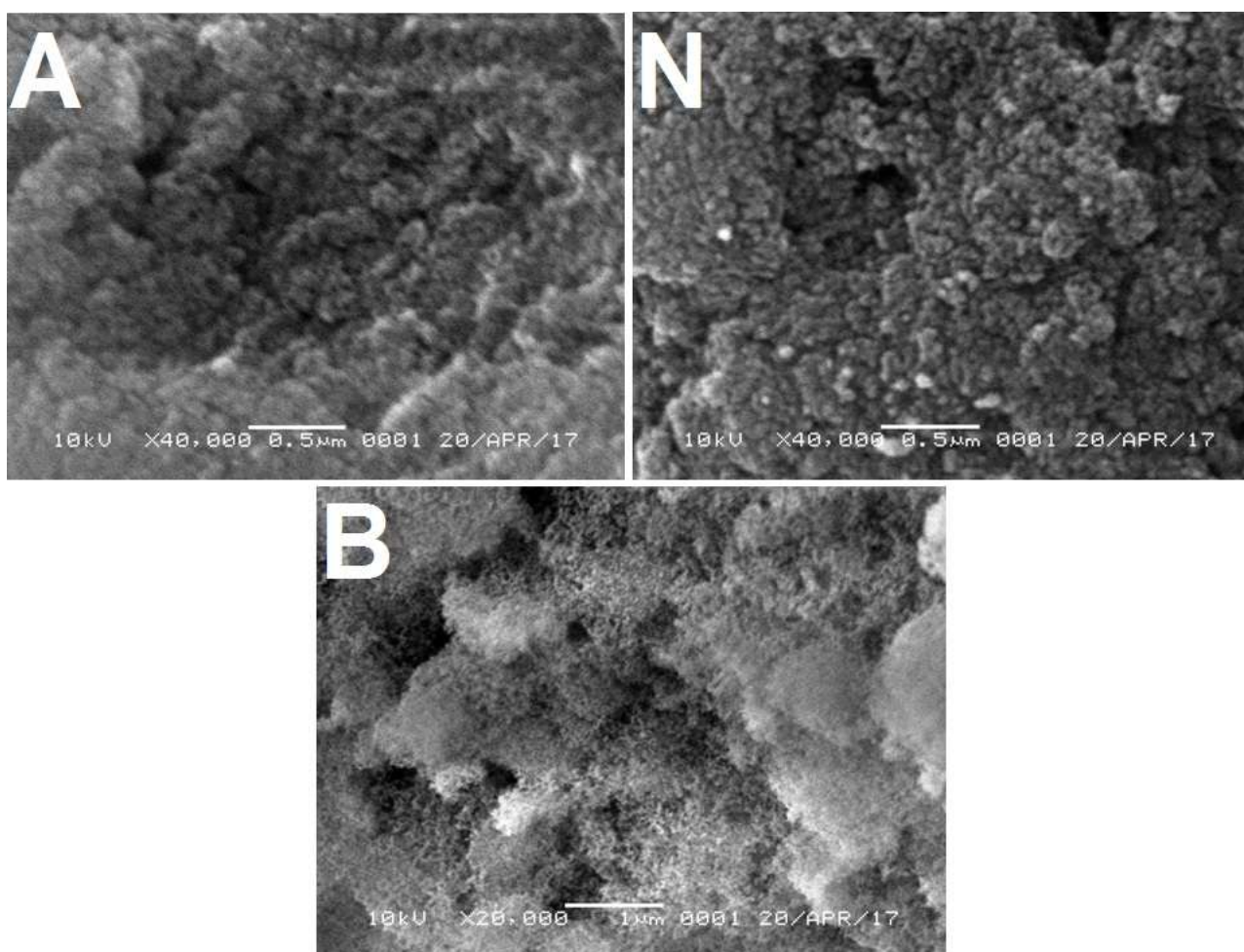


Figure 3: Typical SEM images of precipitated SiO<sub>2</sub> (A) acid; (N) neutral and (B) basic

Table 1  
 Textural characteristics of precipitated SiO<sub>2</sub>

Textural Characteristics	Acid SiO <sub>2</sub>	Neutral SiO <sub>2</sub>	Basic SiO <sub>2</sub>
Specific surface area (m <sup>2</sup> /g)	436	284	84
Total pore volume (cm <sup>3</sup> /g)	0.91	0.74	0.76
Average D pore (nm)	8.4	10.4	36.2

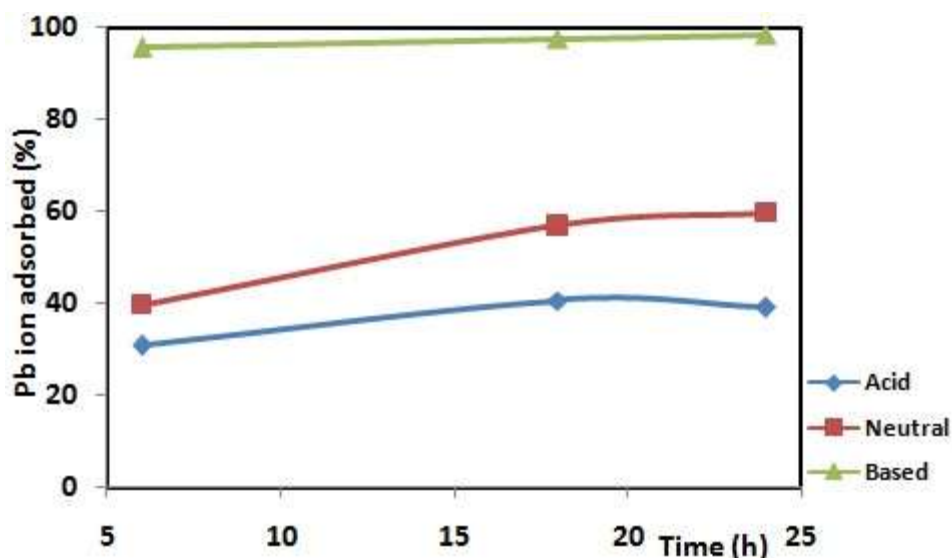


Figure 4: Effect of contact time on adsorption of Pb(II) on acid, neutral and basic precipitated SiO<sub>2</sub>

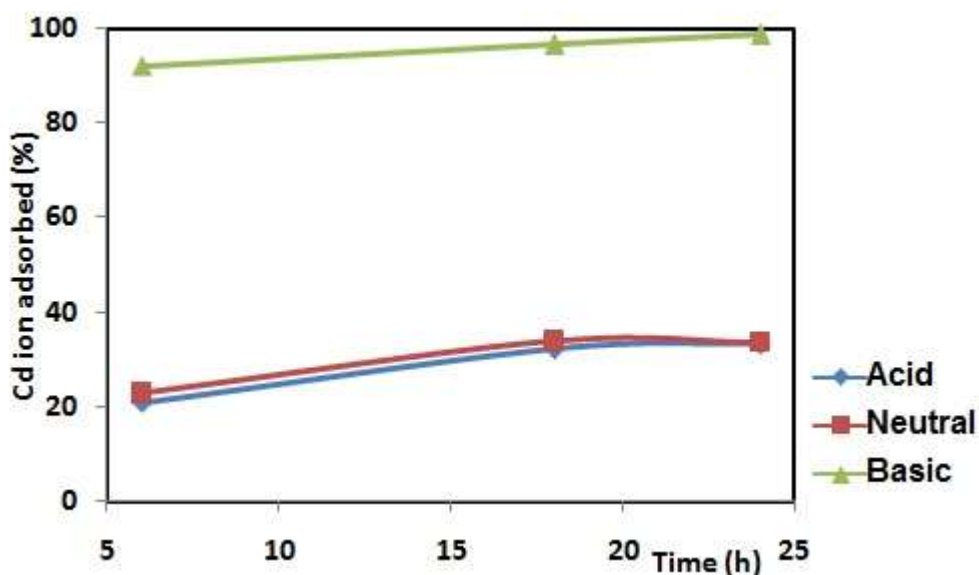


Figure 5: Effect of contact time on adsorption of Cd(II) on acid, neutral and basic precipitated SiO<sub>2</sub>

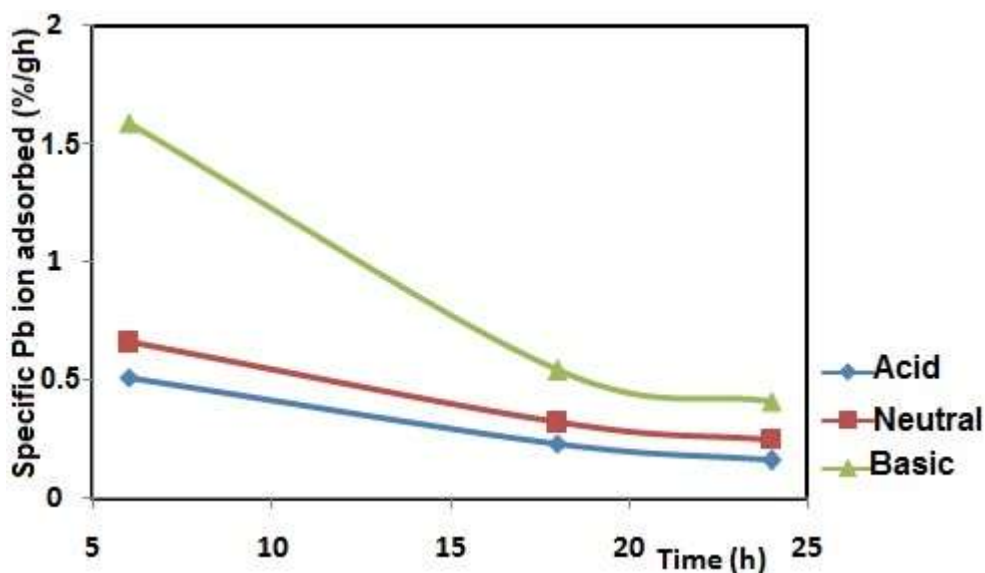


Figure 6: Effect of contact time on specific adsorption of Pb(II) on acid, neutral and basic precipitated SiO<sub>2</sub>

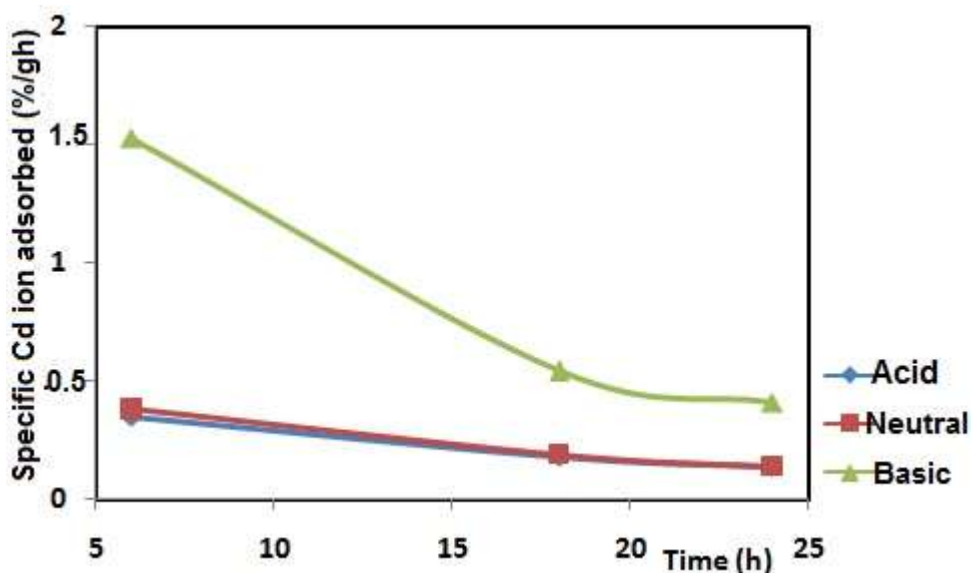


Figure 7: Effect of contact time on specific adsorption of Cd(II) on acid, neutral and basic precipitated SiO<sub>2</sub>

Table 2  
 Heavy metals of Pb adsorption characteristics of precipitated SiO<sub>2</sub>

Adsorbent	Retention time (h)	Concentration of Pb ion Adsorbed (ppm)	Pb ion adsorbed (%)	Specific Pb ion adsorbed (%/gh)
Acid SiO <sub>2</sub>	6	3.747	30.81	0.51
	18	4.949	40.70	0.23
	24	4.747	39.04	0.16
Neutral SiO <sub>2</sub>	6	4.827	39.70	0.66
	18	6.928	56.97	0.32
	24	7.275	59.83	0.25
Basic SiO <sub>2</sub>	6	11.633	95.67	1.59
	18	11.863	97.56	0.54
	24	11.985	98.56	0.41

Table 3  
 Heavy metals of Cd adsorption characteristics of precipitated SiO<sub>2</sub>

Adsorbent	Retention time (h)	Concentration of Cd ion adsorbed (ppm)	Cd ion adsorbed (%)	Specific Cd ion adsorbed (%/gh)
Acid SiO <sub>2</sub>	6	2.987	20.82	0.35
	18	4.619	32.19	0.18
	24	4.779	33.31	0.14
Neutral SiO <sub>2</sub>	6	3.280	22.86	0.38
	18	4.859	33.87	0.19
	24	4.806	33.50	0.14
Basic SiO <sub>2</sub>	6	13.200	92.01	1.53
	18	13.846	96.51	0.54
	24	14.155	98.66	0.41

## Conclusion

The effects of the pH on the amorphous silica characteristics and its capability in the Pb and Cd adsorption were investigated in this study. In this study, the amorphous silica was successfully synthesized from sodium silicate by a precipitation method using sulfuric acid solution at various pH conditions of about 4, 7 and 9. All the silica samples show a low-intensity broad peak at a diffraction angle  $2\theta$  of  $21.8^\circ$  indicating an amorphous structure. The microstructure investigation shows the formation of nanoparticle amorphous silica at all pH conditions.

The basic precipitated silica exhibits the smallest surface area of  $84 \text{ m}^2/\text{g}$ , meanwhile the acidic precipitated silica shows the highest surface area and total pore volumes of  $436 \text{ m}^2/\text{g}$  and  $0.91 \text{ cc/g}$  respectively and the smallest average pore diameter of  $8.4 \text{ nm}$ . However, the basic precipitated silica has the highest percentage adsorption of the Pb(II) and Cd(II) heavy metals of about 98%.

## References

1. Abou Rida M. and Harb F., Synthesis and Characterization of Amorphous Silica Nanoparticles from Aqueous Silicates Using Cationic Surfactants, *J. of Metals, Materials and Minerals*, **24(1)**, 37-42 (2014)
2. Retnaningtyas A.Y., Hidayat R.R., Qomariyah L., Widiyastuti, Kusdianto and Winardi S., The Effect of pH to Drying Process of Colloidal Silica Using Flame Spray Combustor, National Seminar of Chemical Engineering, Yogyakarta Indonesia (2017)
3. Sadeghi M., Dorodian M. and Rezaei M., Synthesis and Characteristic of Precipitated Nano-Silica, *J. of Adv. in Chem.*, **6(1)**, 917-922 (2013)
4. Wilhelm S. and Kind M., Influence of pH, Temperature and Sample Size on Natural and Enforced Syneresis of Precipitated Silica, *Polymers*, **7**, 2504-2521 (2015)
5. Musić S., Filipović-Vinceković N. and Sekovanić L., Precipitation of Amorphous  $\text{SiO}_2$  Particles and Their Properties, *Brazilian J. of Chem. Eng.*, **28(1)**, 89-94 (2011)
6. Wilhelm S. and Kind M., On the Relation between Natural and Enforced Syneresis of Acidic Precipitated Silica, *Polymers*, **6**, 2896-2911 (2014)
7. Mujkanović A., Petrovski P., Vasiljević L. and Ostojić G., The Influence of Precipitation Temperature on Silica Morphology, 14<sup>th</sup> International Research/Expert Conference, TMT 2010, Mediterranean Cruise, 11-18 Sept. (2010)
8. Ying-Mei X., Ji Q., De-Min H., Dong-Mei W., Hui-Ying C., Jun G. and Qiu-Min Z., Preparation of amorphous silica from oil shale residue and surface modification by silane coupling agent, *Oil Shale*, **27(1)**, 37-46 (2010)
9. Geetha D., Ananthiand A. and Ramesh P.S., Preparation and Characterization of Silica Material from Rice Husk Ash- An Economically Viable Method, *Research & Reviews: J. of Pure and Applied Phys.*, **4(3)**, 20-26 (2016)
10. Le V.H., Thuc C.N.H. and Thuc H.H., Synthesis of silica nanoparticles from Vietnamese rice husk by sol-gel method, *Nanoscale Research Letters*, **8(58)**, 1-10 (2013)
11. Contreras C.A., Sugita S. and Ramos E., Preparation of sodium aluminate from basic aluminium sulfate, *The Azo J. of Materials Online*, **2**, 1-18 (2006)
12. Hamouda A.A. and Amiri H.A.A., Factors affecting alkaline sodium silicate gelation for in-depth reservoir profile modification, *Energies*, **7**, 568-590 (2014)
13. Luyten J., Mullens S. and Thijs I., Designing with pores – synthesis and applications, *KONA Powder and Particle Journal*, **28**, 131-142 (2010)
14. Mohapatra M., Khatun S. and Anand S., Adsorption behaviour of Pb(II), Cd(II) and Zn(II) on NALCO plant sand, *Indian J. of Chem. Tech.*, **16**, 291-300 (2009)
15. Xu L., Zheng X., Cui H., Zhu Z., Liang J. and Zhou J., Equilibrium, kinetic and thermodynamic studies on the adsorption of cadmium from aqueous solution by modified biomass ash, Hindawi Publishing Corporation, Bioinorganic Chemistry and Application, 1-9 (2017)
16. Cides da Silva L.C., dos Santos L.B.O., Abate G., Cosentino L.C., Fantini M.C.A., Masini J.C. and Matos J.R., Adsorption of  $\text{Pb}^{2+}$ ,  $\text{Cu}^{2+}$  and  $\text{Cd}^{2+}$  in FDU-1 silica and FDU-1 silica modified with humic acid, *Microporous and Mesoporous Materials*, **110**, 250-259 (2008).